Kono SJ, Ohshima Y, Hoshi K, Bonewald LF, Oda H, Nakamura K, Kawaguchi H, and Tanaka S	Erk pathways negatively regulate matrix mineralization.	Bone	40	68-74	2007
Fijita T, Orimo H, Inoue T, Kaneda K, Sakurai M, Morita R, Yamamoto K, Sugioka Y, Inoue A, Takaoka K, Yamamoto I, Hoshino Y, and Kawaguchi H	Clinical effect of bisphosphonate and vitamin D on osteoporosis: reappraisal of a multicemter double-blind clinical trial comparing etidronate and alfacalcidol.	J Bone Miner Metab	25	130-137	2007
Kawaguchi H, Jingushi S, Izumi T, Fukunaga M, Matsushita T, Nakamura T, Mizuno K, Nakamura T, and Nakamura K	Local application of recombinant human fibroblast growth factor-2 on bone repair: a dose-escalation prospective trial on patients with osteotomy.	J Orthop Res	25	480-487	2007
J. -S. Park, Y. Akiyama, Y. Yamasaki, K. Kataoka	Preparation and characterization of polyion complex micelles with a novel thermosensitive poly(2-isopropyl-2-oxazoline) shell via the complexation of oppositely charged block ionomers.	Langmuir	23 (1)	138-146	2007
Kanis JA, Oden A, Johnell O, Johansson H, De Laet C, Brown J, Burckhardt P, Cooper C, Christiansen C, Cummings S, Eisman JA, Fujiwara S, Gluer C, Goltzman D, Hans D, Krieg MA, La Croix A, McCloskey E, Mellstrom D, Melton LJ III, Pols H, Reeve J, Sanders K, Schott M, Silman A, Torgerson D, van Staa T, Watts NB, Yoshimura N	The use of clinical risk factors enhances the performance of BMD in the prediction of hip and osteoporotic fractures in men and women	Osteoporos Int		in press	2007
佐粧孝久, 中川晃一, 鈴木昌彦, 田原正道, 落合信靖, 荻野修平, 守屋秀繁, 他.	MRIを用いた変形性膝関節症の客観的な重症度評価指数の確立	日本整形外科学会雑誌	81	29-35	2007

福井尚志	変形性関節症の病態：Overviewと最近の知見. 変形性関節症の病態解明・診断・治療の新世紀	日本整形外科学会雑誌	81	5-16	2007
福井尚志	変形性関節症の発症原因. シンポジウム 変形性関節症—最近の進歩.	臨床整形外科	42	17－22	2007
Kyomoto M, Iwasaki Y, Moro T, Konno T, Miyaji F, Kawaguchi H, Takatori Y, Nakamura K, and Ishihara K	High lubricious surface of cobalt-chromium-molybdenum alloy prepared by grafting poly(2-methacryloyloxyethyl phosphorylcholine).	Biomaterials			in press
Saito T, Ikeda T, Nakamura K, Chung UI, and Kawaguchi H	S100A1 and B, transcriptional targets of SOX trio, inhibit terminal differentiation of chondrocytes.	EMBO Rep			in press
Ohba S, Ikeda T, Kugimiya F, Yano F, Lichtler AC, Nakamura K, Takato T, Kawaguchi H, and Chung UI	Identification of a potent combination of osteogenic genes for bone regeneration using embryonic stem (ES) cell-based sensor.	FASEB J			in press
Kawaguchi H	Reverse and forward genetic approaches to the pathophysiology of osteoporosis.	Geriatr Gerontol Int			in press
Kyomoto M, Moro T, Konno T, Takadama H, Yamawaki N, Kawaguchi H, Takatori Y, Nakamura K, and Ishihara K	Enhanced wear resistance of modified cross-linked polyethylene by grafting with poly(2-methacryloyloxyethyl phosphorylcholine).	J Biomed Mater Res A			in press
Kyomoto M, Moro T, Konno T, Takadama H, Kawaguchi H, Takatori Y, Nakamura K, Yamawaki N, and Ishihara K	Effects of photo-induced graft polymerization of 2-methacryloyloxyethyl phosphorylcholine on physical properties of cross-linked polyethylene in artificial hip joints.	J Mater Sci-Mater M			in press
福井尚志	変形性関節症の進行機序に関する最近の知見	関節外科			in press

Ⅳ. 研究成果の刊行物・別刷

Biological Chemistry

DOI: 10.1002/anie.200504441

Intracellular Inducible Alkylation System That Exhibits Antisense Effects with Greater Potency and Selectivity than the Natural Oligonucleotide**

*Md. Monsur Ali, Motoi Oishi, Fumi Nagatsugi, Kenya Mori, Yukio Nagasaki, Kazunori Kataoka, and Shigeki Sasaki**

Synthetic oligonucleotides (ODNs) that incorporate a chemically reactive appendage have been widely investigated in the endeavor to create new functions through specific reactivity toward a target sequence. A number of biotechnological approaches have been invented based on sequence-selective alkylation,[1] cross-linking,[2,3] strand cleavage,[4–7] chemical ligation,[8] signal amplification,[9] and other techniques. Cross-linking oligonucleotides have been used to stabilize complexes with the cellular target mRNA by covalent-bond formation, and have been shown to be useful in enhancing antisense effects. Emerging knowledge about the fundamental role of micro-RNAs (miRNAs) in gene regulation has led to great interest in efficient antisense oligonucleotides against miRNAs as a tool for specifically knocking down particular miRNAs.[10,11] Psoralen derivatives are activated by UV irradiation and are the only reagents applicable to in vitro and in vivo studies. They not only enhance antisense effects[12,13] but also induce specific mutations at the sites of the reaction within the triplex DNA.[14,15] However, until now the use of alkylating oligonucleotides in biological studies has been hampered by the lack of an efficient cross-linking agent. As alkylating or cross-linking agents tend to be unstable under physiological conditions, the use of stable precursors with inducible reactivity was expected to provide a solution to this problem.[2,16] We recently proposed a new concept of inducible reactivity, in which a phenylsulfide derivative used as a stable precursor to a 2-amino-6-vinylpurine nucleoside analogue is automatically activated in the proximity of the target cytidine residue to form a covalent bond selectively (Scheme 1).[17–20] The selectivity of this inducible alkylation system for cytidine is so high that a single nucleotide difference can be discriminated in the alkylation. Herein we describe the capacity of the inducible alkylation system to exhibit antisense effects in an intracellular environment with greater potency and selectivity than the corresponding unmodified oligonucleotide.

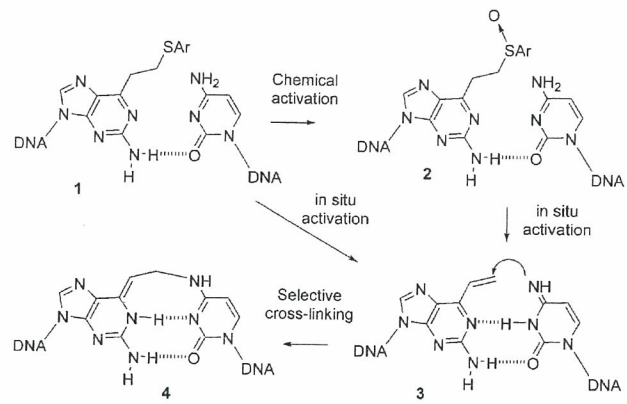

Scheme 1. In situ activation of the sulfide precursor **1** to the 2-amino-6-vinylpurine **3** for selective cross-linking with cytidine to give **4**.[17] The vinyl compound **3** can be generated selectively in the hybrid with the complementary sequence from the sulfoxide **2** or the sulfide precursor **1**. As intermediary formation of **2** has not been detected, it is anticipated that activation from **1** to **3** takes place directly.

In a previous study, the phenylsulfide derivative **1** was oxidized chemically to produce the sulfoxide derivative **2**, which was activated selectively to the vinyl compound **3** by hybridization with the complementary sequence. It has been shown that the cytidine residue at the target site enhances the elimination step from **2** to **3**, which is followed by efficient

[*] Dr. M. M. Ali, Prof. Dr. F. Nagatsugi, Prof. Dr. S. Sasaki
Graduate School of Pharmaceutical Sciences
Kyushu University
3-1-1 Maidashi, Higashi-ku, Fukuoka 812-8582 (Japan)
Fax: (+81) 92-642-6615
E-mail: sasaki@phar.kyushu-u.ac.jp
Dr. M. Oishi, Prof. Dr. Y. Nagasaki
Institute of Materials Science
Tsukuba University
1-1-1 Ten-nodai, Tsukuba, Ibaraki 305–8573 (Japan)
Dr. K. Mori
GeneAct Ltd.
2432-3 Kawaimachi, Kurume, Fukuoka 839-0861 (Japan)
Prof. Dr. K. Kataoka
Department of Materials Science and Engineering
Graduate School of Engineering
The University of Tokyo
7-3-1 Hongo, Bunkyo-ku, Tokyo 113-8656 (Japan)

[**] This work was supported by a Grant-in-Aid for Scientific Research (A) from the Japan Society for the Promotion of Science (JSPS) and CREST of the Japan Science and Technology Agency (JST).

Supporting information for this article is available on the WWW under http://www.angewandte.org or from the author.

alkylation to produce **4**.[17] The vinyl compound **3** can also be generated selectively from the sulfide precursor **1** in the hybrid with the complementary sequence. In this case it is anticipated that activation from **1** to **3** takes place directly. The elimination of the sulfide group is also accelerated by the cytidine residue at the target site. As the sulfide derivative **1** is chemically stable, we viewed it as a potential candidate for an alkylating agent with inducible reactivity for use in living systems.

Herein, we have applied polyion-complex (PIC) micelles of PEG conjugates of oligonucleotides for both the protection of ODNs from enzymatic digestion and their efficient delivery into the cellular interior.[21–23] Scheme 2 summarizes the

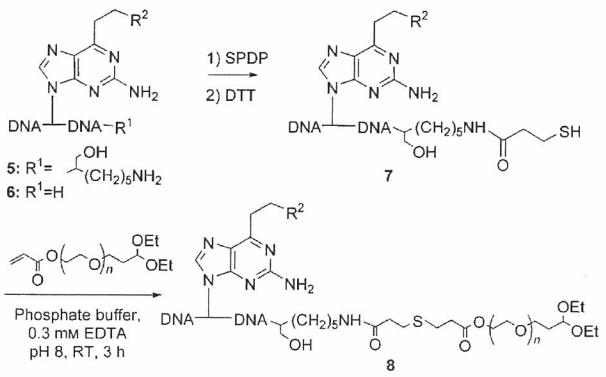

Substituent R^2

a: SMe
b: SPh
c: SC_6H_4-2-COOH
d: SC_6H_4-4-COOH
e: NHPh

Target sequence of firefly luciferase mRNA:
- 3' (446) TACGGGTATGA-C-AACTCGTTA (426) -

Synthesized ODN sequences:
A: 5' ATGCCCATACT-X-TTGAGCAAT
B: 5' ATGCCCATACT-G-XTGAGCAAT
C: 5' GCATAGCGTACT-X-TCTAACTA
X=2-amino 6-alkyl purine (2AP) or G

Scheme 2. Synthesis of the antisense PEG conjugates in which 2-amino 6-alkyl purine is incorporated. The sequence **A** has X at the complementary site to the cytidine residue of the target mRNA sequence, **B** contains X at the adjacent site, and **C** is a random sequence. The description **6A** refers to species with the ODN sequence **A** that are not conjugated with PEG; **8B** (X = AP, R^2 = SMe) is the PEG conjugate with the ODN sequence **B** in which a 2-amino-6-(2-methylthioethyl)purine derivative is incorporated adjacent to the complementary site to the cytidine residue of the target sequence. EDTA = ethylenediaminetetraacetic acid.

synthesis of PEG conjugates of the functional oligonucleotides. The antisense sequence to firefly-luciferase mRNA (sequence **A** in Scheme 2) was designed according to a reported technique.[24] The methylsulfide derivative of a 2-amino 6-alkyl purine was incorporated into the natural-type ODN (**5a** and **6a**),[17] and was then transformed into the phenylsulfide (**5b**, **6b**), 2-carboxyphenylsulfide (**5c**, **6c**), 4-carboxyphenylsulfide (**5d**, **6d**), and phenylamino derivatives (**5e**) by sequential reactions with magnesium monoperphthalate (MMPP) and aqueous NaOH, following the addition of the corresponding thiol or amine. The amino group of the 3′ terminus of **5** was modified with *N*-succimidyl-3-(2-pyridyldithio)propionate (SPDP), followed by reduction with dithiothreitol (DTT) to form the thiol-containing ODN **7**. Finally, the β-thiopropionate linkage of the corresponding ODN–PEG conjugates **8** was formed by a Michael reaction with a PEG polymer bearing a diethylacetal group at one terminus and an acrylate group at the other (M_n = 4460). The conjugates **8** were isolated in good yields by purification by reversed-phase column chromatography. Sequence **A** has X at the complementary site to the cytidine residue of the target mRNA sequence, **B** contains X at the adjacent site, and **C** is a random sequence. The structures of the ODNs and the PEG conjugates were confirmed by MALDI-TOF MS. The PEG–ODN conjugates obtained were mixed with poly-L-lysine (PLL) in a 1:1 molar ratio with respect to the phosphate group in the PEG–ODN conjugate and the amino group in PLL to form the PIC micelles (N/P = 1).

Antisense effects of the reactive ODNs (**6A**, R^1 = H) were first evaluated in a transcription and translation assay without cells. The following order was found for the cross-linking rates of the derivatives of 2-aminopurine in the nonbiological system: phenyl sulfoxide > 2-carboxyphenylsulfide ≫ phenylsulfide > methylsulfide.[17] However, as the phenyl sulfoxide derivatives were found to be unstable in the biological assay, the sulfide-functionalized ODNs were used in this study. Transcription, followed by translation, of firefly luciferase was performed by using ODN **6** (X = G or a sulfide derivative of 2-aminopurine) and firefly-luciferase DNA in a wheat-germ extract. Production of luciferase was monitored by measuring luminescence (Figure 1). All ODNs **6A** showed dose-dependent antisense inhibition. It should be noted that all sulfide-functionalized ODNs showed higher antisense effects than the corresponding natural antisense ODN.

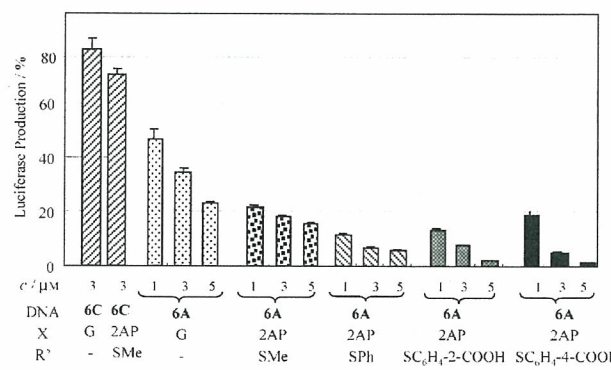

Figure 1. Antisense effects on luciferase production in an assay without cells. Transcription and translation were performed in vitro for 90 min at 30 °C by using DNA (0.3 μg) in the absence or presence of the ODN in TNT coupled wheat germ extract system (Promega). The extent of luciferase production relative to that in the control is shown in the ordinate.

To check whether or not in situ activation would take place in a cell lysate, we mixed the reactive ODN **6A** (X = AP, R^2 = SMe) and the ODN with the target sequence in a cell lysate, and the reaction mixture was analyzed by HPLC.[25] Although the cross-linked adduct was not detected clearly, the formation of 2-amino-6-vinylpurine was evidenced by its intrinsic fluorescence. This vinyl derivative of ODN **6** was

only clearly observed in the presence of the ODN with the target cytidine, which suggests that the activation is dependent on cytidine.

The biological stability of the ODNs was investigated in a cell lysate and in the presence of DNase I. It was shown that the modified ODN **6A** (X = AP, R^2 = SMe) was slightly more stable than the natural ODN **6A** (X = G), and that the PEG conjugate **8A** (X = G) exhibits high stability in a cell lysate (Figure 2a). To rule out the possibility that the higher activity

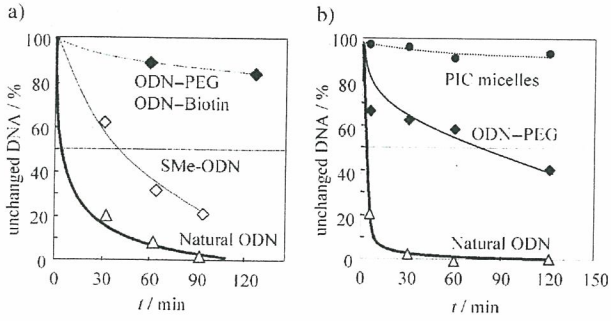

Figure 2. Comparison of the stability of the ODN derivatives in a cell lysate (a) and in the presence of DNase I (b) at 30 °C. Natural ODN: **6A** (X = G), SMe-ODN: **6A** (X = AP, R^2 = SMe), ODN–PEG: **8A** (X = G), ODN–biotin: biotin amide of **5A** (X = G), PIC micelles: B-PEI + **8A** (X = G) (N/P = 1; B-PEI: M_w = 25000, DP = 580). B-PEI = branched polyethyleneimine, DP = degree of polymerization.

of the modified ODNs is merely an effect of higher biostability induced by the modification, we next investigated the antisense effect of the PEG conjugates. The ODN–PEG conjugates were incubated with mRNA of firefly luciferase for 30 min in a buffer, and translation was performed by treatment with an amino acid mixture in a cell lysate for 90 min at 30 °C. It was clearly demonstrated that the PEG conjugate with the modified ODN, **8A** (X = 2AP, R^2 = SMe), exhibited a higher inhibitory effect than the conjugate with the natural ODN, **8A** (X = G), and that the biostability of the modified ODN is not a major factor in the enhancement of the antisense effect.[25]

Hybridization of the ODN with the luciferase mRNA following a cross-linking reaction was next investigated by reverse-transcription polymerase chain reaction (RT-PCR). When primers were used for the upstream and downstream regions of the antisense target site, it was expected that the PCR with cross-linked mRNA would produce shorter PCR products than that with unmodified mRNA. First, ODN **6A** (X = G or 2AP, R^2 = SPh) was mixed with mRNA in a buffer, the mixture was subjected to RT-PCR, and the products were analyzed by gel electrophoresis (Figure 3). The RT-PCR products corresponding to a 223-mer nucleotide of the full length were formed as the major product (Figure 3, lanes 2 and 3), thus indicating that neither covalent nor noncovalent hybridized complexes were formed effectively in a buffer. We next attempted to form complexes with mRNA in cell lysates, so that we could isolate the complexes by using streptavidin affinity beads. mRNA and biotin-conjugated ODN were incubated in a cell lysate, and the hybridized complexes were separated with streptavidin beads. (**5A**–biotin is as biostable

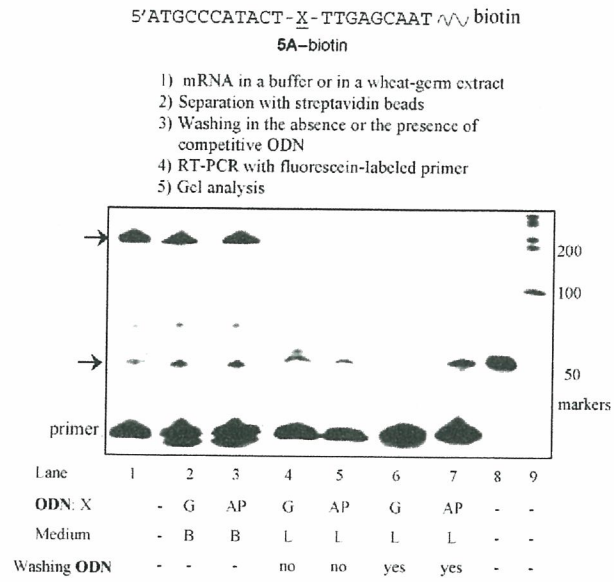

Figure 3. Analysis of RT-PCR products (denoted by arrows) of the reaction of the ODN and luciferase mRNA. Lane 1: control; lane 2: ODN **6A** (X = G) and mRNA were subjected to RT-PCR; lane 3: ODN **6A** (X = 2AP, R^2 = SPh) was used in the same procedure as that for lane 2; lane 4: ODN **5A**–biotin (X = G) and mRNA complexes were separated with streptavidin beads then washed several times with a buffer in the absence of the competitive ODN; lane 5: ODN **5A**–biotin (X = 2AP, R^2 = SPh) was used in the same procedure as that for lane 4; lane 6: washing was done in the presence of the competitive ODN in otherwise the same procedure as that used for lane 4; lane 7: washing was done in the presence of the competitive ODN in otherwise the same procedure as that used for lane 5; lanes 8 and 9: markers. G is guanosine and AP is 2-amino-6-(2-phenylthioethyl)purine (R^2 = SPh; see Scheme 2). Medium B is a buffer and medium L is lysate. The ODN **5A**–biotin has a biotin unit at its 3′ amino end. The sequence of the washing ODN (21 mer) is the sense sequence 3′-TACGGGTATGA-C-AACTCGTTA-5′: the target sequence of firefly-luciferase mRNA.

as the ODN–PEG conjugate, as shown in Figure 2a.) The PCR in which separated streptavidin beads were used afforded shorter RT-PCR products of approximately 50-mer length (Figure 3, lanes 4 and 5), which showed that the RT reaction was inhibited before the site of cross-linking with both the natural ODN (X = G) and the cross-linking ODN (X = 2AP, R^2 = SPh). These results also clearly indicate that tight ODN–mRNA complexes are formed in cell lysates, but not in a buffer, in the case of both the natural and the modified ODN. When the separated streptavidin beads were washed in the presence of the competitive ODN, the short RT-PCR products disappeared in lane 6 and were retained in lane 7, thus demonstrating that covalently bound ODN–mRNA complexes are formed with the cross-linking ODN (X = 2AP, R^2 = SPh). These results, together with the fact that the sulfide derivative is transformed into a 2-amino-6-vinylpurine derivative in cell lysates,[25] strongly suggest that the ODN with the reactive 2-aminopurine residue forms the covalent bond with the target mRNA in the cell lysate to enhance the antisense effect.

We next evaluated the intracellular antisense activity of the reactive ODN–PEG conjugates by a dual-luciferase-

reporter assay. The PIC micelles of the reactive ODN–PEG conjugates exhibit high stability toward enzymatic digestion (Figure 2b) and were therefore used as the system for the delivery of the ODN into the cellular interior.[21,22,25] HuH-7 cells were cotransfected with plasmids of firefly and renilla luciferases in amounts at which both luciferases are expressed to a similar extent. The cells were incubated for 24 h in the presence of the reactive ODN–PEG as the PIC micelles and then for 24 h in a fresh medium. The PEG–ODN conjugates were mixed with PLL (poly-L-lysine, DP = 100, M_w = 20900) with a 1:1 molar ratio of the phosphate group in the PEG–ODN conjugate and the amino group in PLL (N/P = 1) to form the PIC micelles. The luciferase expression was monitored by measuring luminescence with the dual luciferase assay kit. Antisense effects are summarized in Figure 4.

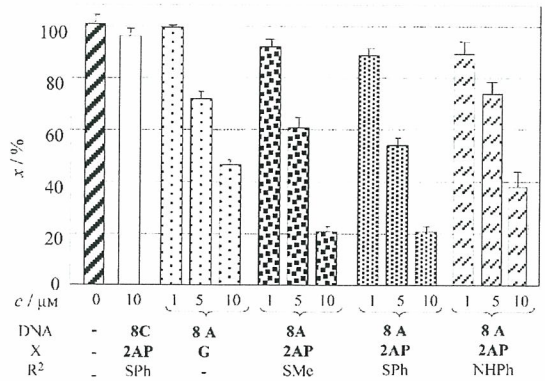

Figure 4. Antisense effects with PEG–ODN/PLL PIC micelles against gene expression of firefly luciferase in cultured HuH-7 cells. Normalized ratios *x* of firefly-luciferase activity to that of renilla luciferase are shown in the ordinate. G and 2AP represent guanosine and the 2-amino 6-alkyl purine nucleoside; substituents R^2 are shown in Scheme 2.

Neither the antisense ODN **6A** nor the PEG–ODN **8A** alone showed antisense inhibition.[21,22] Under conditions under which the PIC micelles of the PEG–ODN **8C** with the random sequence did not show an antisense effect, the micelles of the natural PEG–ODN **8A** clearly showed potent antisense effects of about 50% inhibition at 10 μM. Although higher concentrations of the PIC micelles were needed for potent inhibition than those required in the antisense experiments in cell lysates (compare Figures 1 and 4), the PIC micelles formed with the ODN–PEG conjugates and PLL did not cause cytotoxicity at concentrations of 10 μM.[25] Thus, the inhibitory effects summarized in Figure 4 result from selective antisense effects of **8A**. The sulfide derivatives of 2-aminopurine (**8A**, X = AP, R^2 = SMe and SPh) showed greater antisense effects than the PEG conjugate with the natural antisense oligonucleotide (**8A**, X = G). At a concentration of 10 μM in the sulfide derivative, luciferase expression was inhibited to 20% of that in the control. This degree of expression corresponds to a background level. The ODN containing the aniline derivative (**8A**, X = AP, R^2 = NHPh) was used as an unreactive antisense control. In the presence of this ODN, less effective antisense inhibition was observed, which again supports the hypothesis that the 2-aminopurine derivative in the reactive ODN enhances antisense inhibition.

The consequences of one mismatched site on the antisense effects are compared in Figure 5 for the natural antisense

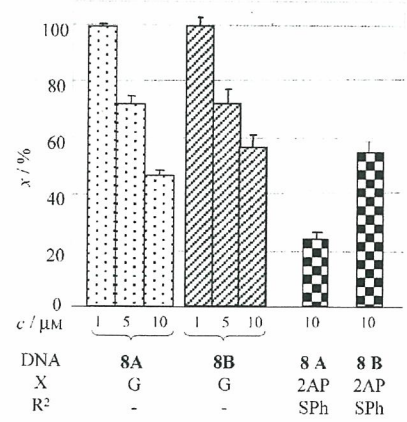

Figure 5. Comparison of the consequences of one mismatched site on the antisense effects. Systems were assayed for their antisense effect in a similar way to that described in the footnote of Figure 4. G and 2AP represent guanosine and the 2-amino 6-alkyl purine nucleoside; substituents R^2 are shown in Scheme 2. *x* = normalized ratios of firefly-luciferase activity to that of renilla luciferase. Target mRNA sequence: -3′-TACGGGTATGA-C-AACTCGTTA-; antisense sequences: **8A**: 5′-ATGCCCATACT-X-TTGAGCAAT-PEG, **8B**: 5′-ATGCCCATACT-G-XTGAG-CAAT-PEG.

ODNs (**8A** and **8B**, X = G) and the reactive ODNs (**8A** and **8B**, X = 2AP, R^2 = SPh). The natural ODN with one mismatched site (**8B**, X = G) exhibited similar inhibition to that of the fully matched ODN (**8A**, X = G), which demonstrates a disadvantage to the use of natural ODNs in terms of antisense inhibition. In marked contrast, the reactive ODN (**8B**, X = AP, R^2 = SPh), in which the 2-aminopurine derivative is at the position adjacent to the target cytidine, was much less efficient than the fully matched ODN (**8A**, X = AP, R^2 = SPh), thus demonstrating the superiority of the reactive ODN over the natural antisense ODN in discriminating a single nucleoside difference in cells. As the 2-amino-6-(2-phenylthioethyl)purine nucleoside is highly selective to cytidine at the complementary position,[17,18] the high sensitivity to a single mismatch site can also be reasonably interpreted as a result of selective cross-linking with the 2-amino-6-vinylpurine derivative.

In this study, we have applied the inducible alkylating system that has been developed by our research group to intracellular antisense oligonucleotides. It was found that the sulfide derivative of the 2-amino-6-vinylpurine nucleoside exhibited high reactivity in a cell lysate, in striking contrast to the chemical reactivity investigated in simple model systems. Detailed investigations of the reaction product of the reactive ODN with mRNA in a cell lysate strongly suggest that the reactive ODN that incorporates the 2-aminopurine nucleoside analogue forms a covalent bond with the target mRNA. The reactive ODN was subsequently applied in intracellular antisense inhibition of luciferase by using polyion-complex

(PIC) micelles of the PEG–ODN conjugate. In conclusion, we have successfully shown that the inducible alkylation system functions in an intracellular environment to promote efficient and selective antisense activity against luciferase production. A unique benefit of this alkylating agent is reflected in its high selectivity, which may permit the discrimination of a single nucleotide difference in cells. As the sulfide precursors to the 2-amino-6-vinylpurine derivative, unlike psoralen, do not need UV irradiation for activation, they are expected to be useful for further in vivo applications. This type of inducible alkylation system combined with the delivery system of PIC micelles for PEG conjugates opens new opportunities for the use of reactive oligonucleotides in vivo.

Received: December 14, 2005
Revised: February 3, 2006
Published online: March 30, 2006

Keywords: alkylation · antisense oligonucleotides · biological chemistry · cross-linking · inducible reactivity

[1] K. B. Grant, P. B. Dervan, *Biochemistry* **1996**, *35*, 12313 – 12319.
[2] For a recent review, see: S. Sasaki, *Eur. J. Pharm. Sci.* **2001**, *13*, 43 – 51; see also references therein.
[3] Q. B. Zhou, S. E. Rokita, *Proc. Natl. Acad. Sci. USA* **2003**, *100*, 15452 – 15457.
[4] Y. Yamamoto, W. Tsuboi, M. Komiyama, *Nucleic Acids Res.* **2003**, *31*, 4497 – 4502.
[5] T. Fukuma, C. M. Walton, C. H. Wu, G. Y. Wu, *Bioconjugate Chem.* **2003**, *14*, 295 – 301.
[6] R. N. Zuckermann, D. R. Corey, P. G. Schultz, *J. Am. Chem. Soc.* **1988**, *110*, 1614 – 1615.
[7] K. Nagai, S. M. Hecht, *J. Biol. Chem.* **1991**, *266*, 23994 – 24002.
[8] S. Sando, H. Abe, E. T. Kool, *J. Am. Chem. Soc.* **2004**, *126*, 1081 – 1087.
[9] M. P. van de Corput, R. W. Dirks, R. P. M. van Gijlswijk, E. van Binnendijk, C. M. Hattinger, R. A. de Paus, J. E. Landegent, A. K. Raap, *J. Histochem. Cytochem.* **1998**, *46*, 1249 – 1259.
[10] G. Meister, M. Landthaler, Y. Dorsett, T. Tuschl, *RNA* **2004**, *10*, 544 – 550.
[11] G. Hutvagner, M. J. Simard, C. C. Mello, P. D. Zamore, *PLoS Biol.* **2004**, *2*, e98.
[12] A. Murakami, A. Yamayoshi, R. Iwase, J. Nishida, T. Yamaoka, N. Wake, *Eur. J. Pharm. Sci.* **2001**, *13*, 25 – 34.
[13] J. M. Kean, A. Murakami, K. R. Blake, D. D. Cushman, P. S. Miller, *Biochemistry* **1988**, *27*, 9113 – 9121.
[14] N. Puri, A. Majumdar, B. Cuenoud, P. S. Miller, M. M. Seidman, *Biochemistry* **2004**, *43*, 1343 – 1351.
[15] A. Majumdar, A. Khorlin, N. Dyatkina, F. L. Lin, J. Powell, J. Liu, Z. Fei, Y. Khripine, K. A. Watanabe, J. George, P. M. Glazer, M. M. Seidman, *Nat. Genet.* **1998**, *20*, 212 – 214.
[16] Q. B. Zhou, S. E. Rokita, *Proc. Natl. Acad. Sci. USA* **2003**, *100*, 15452 – 15457.
[17] T. Kawasaki, F. Nagatsugi, Md. M. Ali, M. Maeda, K. Sugiyama, K. Hori, S. Sasaki, *J. Org. Chem.* **2005**, *70*, 14 – 23.
[18] F. Nagatsugi, T. Kawasaki, D. Usui, M. Maeda, S. Sasaki, *J. Am. Chem. Soc.* **1999**, *121*, 6753 – 6754.
[19] F. Nagatsugi, K. Uemura, S. Nakashima, M. Maeda, S. Sasaki, *Tetrahedron* **1997**, *53*, 3035 – 3044.
[20] F. Nagatsugi, K. Uemura, S. Nakashima, M. Maeda, S. Sasaki, *Tetrahedron Lett.* **1995**, *36*, 421 – 424.
[21] M. Oishi, S. Sasaki, Y. Nagasaki, K. Kataoka, *Biomacromolecules* **2003**, *4*, 1426 – 1432.
[22] M. Oishi, F. Nagatsugi, S. Sasaki, Y. Nagasaki, K. Kataoka, *ChemBioChem* **2005**, *6*, 1 – 6.
[23] For a similar method, see: J. H. Jeong, S. W. Kim, T. G. Park, *Bioconjugate Chem.* **2003**, *14*, 473 – 479.
[24] M. Mishra, J. R. Bennett, G. Chaudhuria, *Biochem. Pharmacol.* **2001**, *61*, 467 – 476.
[25] See the Supporting Information.

Arch Osteoporos
DOI 10.1007/s11657-006-0007-0

ORIGINAL ARTICLE

Cumulative incidence and changes in the prevalence of vertebral fractures in a rural Japanese community: a 10-year follow-up of the Miyama cohort

Noriko Yoshimura · Hirorfumi Kinoshita · Hiroyuki Oka · Shigeyuki Muraki · Akihiko Mabuchi · Hiroshi Kawaguchi · Kozo Nakamura

Received: 28 April 2006 / Accepted: 17 July 2006

Abstract
Introduction The objective of this study was to clarify secular changes in the prevalence and cumulative incidence of vertebral fractures (VFx) among the general inhabitants of Miyama, a rural Japanese community.
Methods A cohort of 1,543 inhabitants aged 40–79 years was established using resident registration in 1989. Of these, 400 participants were selected and divided into four age strata, each containing 50 men and 50 women. Participants completed a self-administered questionnaire and anthropometric measurements were taken. In 1990, baseline radiographic examinations of the thoracolumbar spine in anteroposterior and lateral views were performed. Radiographic examinations of the same sites were performed on the same participants in 2000. All VFx were diagnosed by the same experienced orthopedic surgeon. Evaluation of radiographic surveys after 10 years was completed for 287 of the 400 participants (132 men, 155 women; 71.8%).
Results The prevalences of VFx at follow-up in 2000 for subjects in their 50s, 60s, 70s, and 80s were 2.9%, 10.3%, 13.2%, and 25.0% for men, and 2.1%, 9.1%, 20.5%, and 54.2% for women, respectively. Prevalence in the present study was compared with that collected in 1990, showing improvements over time for men and women in their 50s, 60s, and 70s. Future problems with osteoporotic fractures in Japan might, thus, be less severe than previously predicted. Cumulative incidence over 10 years was detected by the number of incident cases divided by the number of all participants in the initial study. Incident cases were defined by two criteria. First, cases with prevalent VFx were excluded from both the numerators and the denominators. In this analysis, the cumulative incidence of the cases with first VFx was detected. Secondly, the cumulative incidence including the subjects who had suffered from the prevalent fractures and with an increased number of VFx in the following 10 years were calculated. This analysis clarified the cumulative incidence of cases with and without previous VFx. Incidence over 10 years of subjects in their 40s, 50s, 60s, and 70s with first VFx were 2.2%, 4.9%, 5.1%, and 10.8% for men, and 2.1%, 4.5%, 14.0%, and 22.2% for women, respectively. By contrast, if new cases were defined as including subjects who had suffered from previous fractures, but displayed an increased number of VFx, cumulative incidences for subjects in their 40s, 50s, 60s, and 70s were 2.1%, 8.3%, 10.0%, and 12.2% for men, and 2.1%, 6.1%, 18.0%, and 22.4% for women, respectively.

Keywords Cohort study · Cumulative incidence · Japanese · Prevalence · Vertebral fractures

N. Yoshimura · H. Oka
Department of Joint Disease Research, 22nd Century Medical and Research Center, Graduate School of Medicine, University of Tokyo, Tokyo, Japan

H. Kinoshita
Department of Orthopaedic Surgery, Wakayama Medical University Kihoku Hospital, Wakayama, Japan

S. Muraki · A. Mabuchi
Department of Clinical Motor System Medicine, 22nd Century Medical and Research Center, Graduate School of Medicine, University of Tokyo, Tokyo, Japan

H. Kawaguchi · K. Nakamura
Department of Orthopaedic Surgery, Faculty of Medicine, University of Tokyo, Tokyo, Japan

N. Yoshimura (✉)
7-3-1 Hongo, Bunkyo-ku, Tokyo 113-8655, Japan
e-mail: yoshimuran-ort@h.u-tokyo.ac.jp

Introduction

Among fractures due to osteoporosis, vertebral fractures (VFx) are the most likely to lead to marked health problems. VFx are reportedly associated with functional impairment [1], back pain [2, 3], kyphosis [2, 3], esophageal reflux [4], depressive mood [5], respiratory dysfunctions [6], and decreased quality of life [7, 8]. In addition, VFx increase the risk of new VFx and hip fractures [9–13]. Furthermore, prevalent VFx reportedly increase mortality risk [14–16].

Although preventive strategies for VFx are urgently needed with the rapid aging of populations such as in Japan, little data is available concerning epidemiological characteristics in population samples, particularly in Japan [17–19]. A population-based cohort was established in 1990, comprising subjects aged 40- to 79-years-old from resident registrations for a village in a mountainous area, Miyama village, and follow-up studies were conducted in 1993, 1997, and 2000 [20–22]. In the previous report of the Miyama study, prevalences of VFx were ascertained for men and women [23].

In the present study, radiographic examination was performed on the same subjects after 10 years to assess secular trends of prevalence and to clarify cumulative incidences among different generations of VFx in a rural Japanese community.

Participants and methods

Epidemiological research based on populations has been conducted in Miyama village, Wakayama prefecture, Japan. As a detailed profile of the Miyama cohort has already been described elsewhere [20–23], a brief summary is provided here. In this village, a list of inhabitants aged 40- to 79-years-old was compiled based on resident registrations as of the end of December 1988. As a result, a cohort of 1,543 inhabitants (716 men, 827 women) was identified. A self-administered questionnaire survey regarding 125 daily activities such as smoking habits, alcohol consumption, and physical exercise was performed (baseline study).

From the above-mentioned cohort, 50 men and 50 women in each decade of age between 40 and 79 years (for a total of 400 participants) was recruited based on resident registrations for the purpose of measuring bone mineral density (BMD) in 1990 (initial BMD survey). In addition to BMD measurements using dual energy X-ray absorptiometry (DXA; Lunar DPX, GE Medical Systems, Madison, WI, USA), an interviewer-administered questionnaire, medical examination, and physical measurements were also performed for these participants. The questionnaire comprised 70 items, such as past history, history of medication, smoking habits, alcohol consumption, calcium intake, physical exercise, history of childbirth, history of lactation, and menstrual status. Radiographic examination of the spine was performed on all participants in 1990. Anteroposterior and lateral images of thoracolumbar vertebrae Th5-L5 were used for diagnosis (initial X-ray survey). Radiographic examination was again performed on subjects who provided consent after 10 years. Lateral images of thoracolumbar vertebrae Th5-L5 were again used for diagnosis (2nd X-ray survey).

Lateral spinal radiographs were examined for the presence of one or more VFx between Th5-L5, using the criteria defined by the Japan Bone and Mineral Society (Fig. 1) [24]. According to these criteria, the measurement of anterior, middle, and posterior heights on lateral radiography of the thoracic and lumbar spine is required, in order to determine ratios defining the anterior wedge, biconcave, and compound dimensions of the vertebral bodies. Diagnosis of VFx on all radiographs was performed by the same experienced orthopedic doctor (HK).

Prevalence and cumulative incidence were calculated by utilizing the results of diagnosis. Cumulative incidence is defined simply as the ratio of incident cases to the at-risk population at the beginning of the observation period. In the present study, cumulative incidence over 10 years was, thus, detected as the number of incident cases divided by the number of all participants in the initial study. Incident cases were defined using two criteria. First, cases with previous VFx were excluded from both numerators and denominators. In this analysis, the cumulative incidence of cases with first VFx was detected. Secondly, the cumulative incidence including subjects who had suffered from previous VFx but who displayed an increased number of VFx over the following 10 years was calculated. This analysis clarified the cumulative incidence of cases with and without previous VFx.

In the above-mentioned formula to obtain the cumulative incidence, the denominator was defined as the total number of participants in the initial X-ray survey. Using this definition, drop-outs during the observed 10 years were considered as non-VFx. To avoid underestimation caused

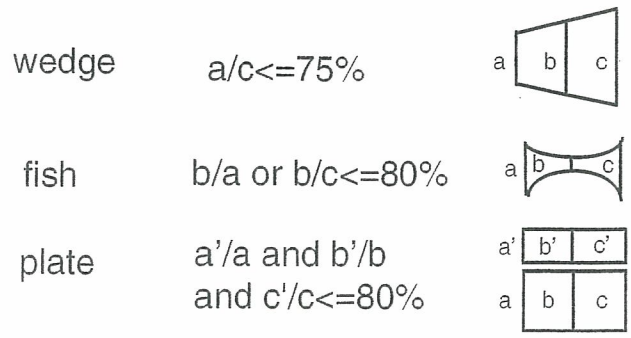

Fig. 1 Diagnostic criteria for vertebral fractures in Japan

by the inclusion of drop-outs, another cumulative incidence was calculated by excluding drop-outs during the study period from the denominator. This index was defined as the cumulative incidence among survivors.

All statistical analyses were performed using STATA statistical software (STATA Corp., College Station, TX, USA).

Results

We note our findings as follows:

1. Eligible participants
   Among 400 participants of the initial BMD examination, 390 provided consent to participate in the radiographic examination (194 men, 196 women; 97.5%) of the initial survey. Radiographic evaluation after 10 years was completed for 287 of the 400 participants (132 men, 155 women; 71.8%). The loss of 101 participants was explained as follows: 55 participants died (37 men, 18 women); 16 participants moved (8 men, 8 women); 13 participants were ill (4 men, 9 women); 8 participants were busy (8 men); 5 participants refused to participate further (5 men); and 4 participants were away from the area at the time of follow-up (1 man, 3 women). Another 12 participants (5 men, 7 women) were excluded from analysis due to the poor quality of radiographic images. Table 1 shows the physical characteristics of the remaining participants at the time of the initial X-ray survey.
2. Prevalence of VFx at the survey in 2000 and secular trends 1990–2000
   The prevalences of VFx at follow-up in 2000 were calculated. The prevalences of VFx for subjects in their 50s, 60s, 70s, and 80s were 2.9%, 10.3%, 13.2%, and 25.0% for men, and 2.1%, 9.1%, 20.5%, and 54.2% for women, respectively.
   Figure 2 shows a comparison of VFx prevalences in the same age group according to the results of radiographic examination in 1990. The prevalences were significantly decreased between the 50s to 70s age groups in 2000 compared to 1990 ($P<0.05$) (Fig. 2).
3. Cumulative incidence of VFx
   The cumulative incidences over 10 years for men and women sorted by the presence or absence of VFx at the

Table 1 Characteristics of participants of the initial survey, classified by sex and age stratum

	Age strata of participants	No. of participants	No. of participants	Anthropometric measurements at the initial survey (mean (SD))				BMD measurements on initial survey (mean (SD))	
Birth cohort	Initial survey 1990	Initial X-ray survey 1990	Follow-up 2000	Age (yrs)	Height (cm)	Weight (kg)	BMI (kg/m^2)	BMD (L2-4)	BMD (femoral neck)
Men	Total	194	132	56.9 (10.3)	161.3 (6.7)	58.2 (9.2)	22.3 (2.5)	1.10 (0.19)	0.88 (0.14)
1940–49	40–49	47	35	44.1 (3.2)	166.3 (5.8)	63.8 (8.4)	23.0 (2.3)	1.18 (0.17)	0.97 (0.15)
1930–39	50–59	48	39	53.9 (2.6)[a]	162.0 (5.8)[a]	60.1 (8.2)	22.8 (2.4)	1.16 (0.18)	0.91 (0.12)
1920–29	60–69	50	38	63.2 (2.8)[ab]	159.4 (5.4)[a]	56.1 (7.5)[a]	22.0 (2.4)	1.03 (0.19)[ab]	0.82 (0.12)[ab]
1910–19	70–79	49	20	73.3 (2.8)[abc]	154.7 (4.8)[abc]	48.7 (6.8)[abc]	20.3 (2.5)[ab]	1.01 (0.16)[ab]	0.79 (0.10)[ab]
Women	Total	196	155	56.7 (10.1)	149.0 (6.0)	49.7 (8.1)	22.3 (2.8)	0.98 (0.23)	0.76 (0.14)
1940–49	40–49	48	48	44.6 (3.0)	152.6 (4.7)	53.6 (8.3)	22.9 (2.8)	1.18 (0.16)	0.88 (0.12)
1930–39	50–59	49	44	54.8 (2.7)[a]	149.9 (5.1)	50.1 (7.1)	22.3 (2.6)	0.99 (0.18)[a]	0.75 (0.12)[a]
1920–29	60–69	50	39	64.3 (2.8)[ab]	147.4 (5.1)[a]	47.5 (6.9)[a]	21.9 (3.0)	0.85 (0.20)[ab]	0.69 (0.11)[a]
1910–19	70–79	49	24	71.6 (1.8)[abc]	142.5 (5.6)[abc]	44.5 (7.6)[ab]	21.9 (3.0)	0.78 (0.16)[ab]	0.64 (0.09)[ab]

[a] Significantly different from values of the birth cohort group born in 1940–49
[b] Significantly different from values of the birth cohort group born in 1930–39
[c] Significantly different from values of the birth cohort group born in 1920–29

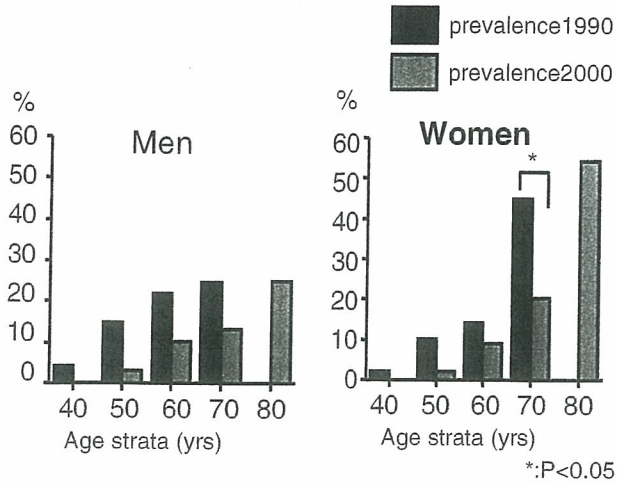

Fig. 2 Comparison of prevalence for vertebral fractures in the same age groups among participants in the X-ray examinations performed in 1990 and 2000

initial X-ray survey are shown in Table 2. The cumulative incidence of VFx including subjects with previous VFx after 10 years increased with age in both men and women.

After excluding cases with previous VFx, the cumulative incidence of first VFx for participants in their 40s, 50s, 60s, and 70s increased with age in both men and women, and was higher in women than in men in all age strata, except the 40s.

Although no association was identified between the cumulative incidence among participants with previous VFx and age in both men and women, cumulative incidence was significantly higher for subjects with previous VFx than for subjects without previous VFx in both men and women ($P<0.05$).

4. Cumulative incidence of VFx among survivors

The cumulative incidences of VFx among cases with first VFx for survivors in their 40s, 50s, 60s, and 70s were 2.9%, 2.8%, 8.6%, and 21.1% for men, and 2.1%, 7.0%, 18.9%, and 31.3% for women, respectively. The cumulative incidence of the first VFx among survivors increased with age in both men and women, and was higher in women than in men in all age strata, except in the 40s.

The cumulative incidences of VFx including subjects who had suffered from previous fractures or with increased numbers of VFx after 10 years for survivors in their 40s, 50s, 60s, and 70s were 2.9%, 10.3%, 13.2%, and 30.0% for men, and 2.1%, 6.8%, 23.1%, and 45.8% for women, respectively, suggesting an increase with age. Cumulative incidence was, again, significantly higher for subjects with previous VFx than for those without previous VFx in both men and women ($P<0.01$).

Discussion

The present study evaluated the prevalence and cumulative incidence of VFx over 10 years using radiographic diagnosis after the performance of two radiographic examinations of the thoracolumbar spine in anteroposterior and lateral views of population-based subjects.

Compared with hip fractures, epidemiological studies of VFx have been less available. One reason for this is the fact that VFx are not always symptomatic, and longitudinal

Table 2 Cumulative incidences over 10 years for men and women classified by the presence or absence of VFx at the initial survey

		All participants			With presence of VFx at the initial survey			With absence of VFx at the initial survey		
Birth cohort	Age strata at the initial survey (yrs)	No. of new VFx 1990–2000	No. of participants initial X-ray survey 1990	Cumulative incidence (%)	No. of new VFx cases 1990–2000	No. of participants initial survey 1990	Cumulative incidence (%)	No. of new VFx cases 1990–2000	No. of participants initial survey 1990	Cumulative incidence (%)
Men	Total	16	194	8.2	7	32	21.9	9	162	5.6
1940–49	40–49	1	47	2.1	0	2	0.0	1	45	2.2
1930–39	50–59	4	48	8.3	2	7	28.6	2	41	4.9
1920–29	60–69	5	50	10.0	3	11	27.3	2	39	5.1
1910–19	70–79	6	49	12.2	2	12	16.7	4	37	10.8
Women	Total	24	196	12.2	9	35	25.7	16	161	9.9
1940–49	40–49	1	48	2.1	0	1	0.0	1	47	2.1
1930–39	50–59	3	49	6.1	1	5	20.0	2	44	4.5
1920–29	60–69	9	50	18.0	3	7	42.9	6	43	14.0
1910–19	70–79	11	49	22.4	5	22	22.7	6	27	22.2

population surveys are required to clarify epidemiological indices. The present study used subjects representative of the whole town, and careful follow-up was performed. One limitation was the use of a relatively small number of fractures and small study population to determine the prevalence and cumulative incidence of VFx. However, few such longitudinal observational studies with high participation rates have been reported, representing the principal strength of this study.

Another reason for the scarcity of data on this subject is the lack consensus regarding the definition of VFx [25]. The present study utilized the diagnostic criteria of the Japan Bone and Mineral Society, as these criteria are the most popular and most commonly used in various clinical fields in Japan. These criteria seem to use the kind of semiquantative (SQ) method advocated by Genant et al. [26]. From the perspective of grading in SQ methods, the criteria of the Japan Bone and Mineral Society correspond to grades above SD2. The epidemiological indices in the present study, thus, did not include cases classifiable as SD1, suggesting that the results obtained using Japanese criteria might represent an underestimation compared to other results diagnosed using SQ methods.

Population-based prevalence studies of VFx have been performed in Western countries, such as the USA [27], Denmark [28, 29], Finland [30], Sweden [31, 32], the Netherlands [33], England [34, 35], and France [36, 37], and in a multicenter study involving 19 European countries [38]. In Asia, the prevalence of VFx has been reported in Taiwan [39], China [40], and Japan [18, 19, 24]. Cummings et al. compared the results of population-based studies of radiological VFx prevalence in women ≥50-years-old between Europe, Minnesota (USA), Hawaii (USA), Hiroshima (Japan), Taiwan, and Beijing (China) [41]. In this comparison, the prevalence of VFx among women >70-years-old was higher in Japan than in the USA or China, and was as high as that in Europe. The prevalence of VFx in the mountainous area of the present study was much higher than that in Hiroshima, an urban area, suggesting that regional differences in VFx might be present in Japan.

The present study clarified differences in the prevalence of VFx for given age strata between birth cohorts. The comparison of data collected in 1990 and 2000 showed improvements over time for men and women in their 50s, 60s, and 70s. A previous report has already noted that BMD data from 1990 and 2000 showed significant improvements for men in their 60s and for women in their 50s [23], concluding that this might predict a decrease in the prevalence of osteoporosis in the near future in Japan. The present results suggest that the prevalence of not only osteoporosis, but also osteoporotic fractures, could decrease in the future in Japan. Fujiwara et al. assessed the effects of birth cohort on the incidence of VFx in Hiroshima, and reported that incidence decreased by a factor of 0.5 in men and 0.6 in women with each succeeding birth decade [17]. The present data are consistent with these findings.

This low prevalence of VFx in more recent birth cohorts may reflect nutritional improvements, in addition to BMD improvements. As noted elsewhere [23], nationwide nutritional surveys have reported the mean calcium intake as 253 mg/day in 1946 (1st survey), 338 mg/day in 1955, 465 mg/day in 1965, and 552 mg/day in 1975 [42], representing a dramatic increase. These nutritional improvements might be expected to increase body build and BMD, and, thus, decrease the prevalence of VFx in all age groups. Another possible reason for the decreasing prevalence of VFx might be the effects of action taken for the prevention of osteoporosis by the government and academic societies. To achieve the prevention of osteoporosis, the Ministry of Health, Labour and Welfare recommended all that communities start BMD screening for middle-aged and elderly female residents in 1995. These examinations in various communities have enabled many women to become more aware of osteoporosis. Moreover, the Japan Osteoporosis Foundation and the Japan Osteoporosis Society, which were established in 1991 and 1999, respectively, have been conducting public education campaigns to inform the general population about osteoporosis and risk factors. These efforts by both the government and academic societies might have resulted in the decreasing prevalence of VFx.

Regarding the incidence of VFx, while some epidemiological studies have been reported from Western countries [43–45], the only investigation from Japan was reported by Fujiwara et al. [18]. Fujiwara et al. performed radiographic examinations in 1994–1995, with follow-up at an average of 4 years, and clarified the incidence of VFx in their Hiroshima cohort. Incidences of VFx in this Hiroshima cohort increased with age, particularly after about 60 years of age, and women displayed a nearly two-fold greater incidence of VFx than men. The incidence of VFx was much higher in individuals with previous VFx than in those without previous VFx. As cumulative incidence was clarified in the present study, rather than incidence, direct comparison of the present results with those of Fujiwara et al. might be incorrect. However, findings in the present study, such as age-dependency, sex differences, and higher incidence in individuals with previous VFx than in those without previous VFx, are consistent with the results of the previous investigation in Hiroshima.

The cumulative incidence for participants at the initial survey in the present study could be considered as a 10-year probability according to age. In this mountain village, 12.2% of men and 22.4% of women in their 70s will suffer new morphometric VFx in the next 10 years. Kanis et al. reported the 10-year probability of clinical VFx in female

participants in the European Prospective Osteoporosis Study [46]. The 10-year probability of clinical VFx among women with a 0 Z-score of amplitude-dependent speed of sound on quantitative ultrasound (QUS) measurements was 3.9% at 70 years old, 4.5% at 75 years old, and 4.9% at 80 years old. Although only about one-third of morphometric fractures reportedly come to medical attention [43], the present results indicated much higher incidences than those described by Kanis et al. Although the future incidence of VFx in the Japanese population could be predicted to decrease, elderly individuals seem to remain at high risk. To reduce the incidence and prevalence of osteoporosis and osteoporotic fractures, further epidemiological research is needed to facilitate the development of affordable strategies for the early identification of high-risk individuals.

Acknowledgments This work was supported by Grants-in-Aid for Scientific Research C16590512 from the Ministry of Education, Science, Sports, and Culture in Japan, H16-Chihou Kossetsu-021, H17-Meneki-009 from the Ministry of Health, Labour and Welfare, and the grant from the Japan Osteoporosis Society.

References

1. Burger H, Van Daele PL, Grashuis K, Hofman A, Grobbee DE, Schutte HE, Birkenhanger JC, Pols HA (1977) Vertebral deformities and functional impairment in men and women. J Bone Miner Res 12(1):152–157
2. Ross PD (1977) Clinical consequences of vertebral fractures. Am J Med 103(2A):30S–43S
3. Nevitt MC, Ettinger B, Black DM, Stone K, Jamal SA, Ensrud K, Segal M, Genant HK, Cummings RS (1988) The association of radiographically detected vertebral fractures with back pain and function: a prospective study. Ann Intern Med 128(10):793–800
4. Yamaguchi T, Sugimoto T, Yamada H, Kanzawa M, Yano S, Yamauchi M, Chihara K (2002) The presence and severity of vertebral fractures is associated with the presence of esophageal hiatal hernia in postmenopausal women. Osteoporos Int 13(4):331–336
5. Gold DT, Lyles KW, Shipp KM, Drezner MK (2001) Osteoporosis and its nonskeletal consequences: their impact on treatment decisions. In: Marcus R, Feldman D, Kelsey J (eds) Osteoporosis, 2nd edn. Academic Press, San Diego, California, pp 819–829
6. Leech JA, Dulberg C, Kellie S, Pattee L, Gay J (1990) Relationship of lung function to severity of osteoporosis in women. Am Rev Respir Dis 141(1):68–71
7. Gold DT (1966) The clinical impact of vertebral fractures: quality of life in women with osteoporosis. Bone 18(3 Suppl):185S–189S
8. Oleksik A, Lips P, Dawson A, Minshall ME, Shen W, Cooper C, Kanis J (2000) Health-related quality of life in postmenopausal women with low BMD with or without prevalent vertebral fractures. J Bone Miner Res 15(7):1384–1392
9. Ross PD, Davis JW, Epstein RS, Wasnich RD (1991) Pre-existing fractures and bone mass predict vertebral fracture incidence in women. Ann Intern Med 114(11):919–923
10. Ross PD, Genant HK, Davis JW, Miller PD, Wasnich RD (1993) Predicting vertebral fracture incidence from prevalent fractures and bone density among non-black, osteoporotic women. Osteoporos Int 3(3):120–126
11. Nevitt MC, Ross PD, Palermo L, Musliner T, Genant HK, Thompson DE (1999) Association of prevalent vertebral fractures, bone density, and alendronate treatment with incident vertebral fractures: effect of number and spinal location of fractures. The Fracture Intervention Trial Research Group. Bone 25(5):613–619
12. Black DM, Arden NK, Palermo L, Pearson J, Cummings SR (1999) Prevalent vertebral deformities predict hip fractures and new vertebral deformities but not wrist fractures. Study of Osteoporotic Fractures Research Group. J Bone Miner Res 14 (5):821–828
13. Burger H, van Daele PLA, Algra D, Hofman A, Grobbee DE, Schutte HE, Birkenhager JC, Pols HA (1994) Vertebral deformities as predictors of non-vertebral fractures. BMJ 309:991–992
14. Center JR, Nguyen TV, Schneider D, Sambrook PN, Eisman JA (1999) Mortality after all major types of osteoporotic fracture in men and women: an observational study. Lancet 353(9156):878–882
15. Ensrud KE, Thompson DE, Cauly JA, Nevitt MC, Kado DM, Hochberg MC, Santora AC 2nd, Black DM (2000) Prevalent vertebral deformities predict mortality and hospitalization in older women with low bone mass. Fracture Intervention Trial Research Group. J Am Geriatr Soc 48(3):241–249
16. Johnell O, Kanis JA, Oden A, Sernbo I, Redlund-Johnell I, Petterson C, De Laet C, Jonsson B (2004) Mortality after osteoporotic fractures. Osteoporos Int 15(1):38–42
17. Fujiwara S, Mizuno S, Ochi Y, Sasaki H, Kodama K, Russell WJ, Hosoda Y (1991) The incidence of thoracic vertebral fractures in a Japanese population, Hiroshima and Nagasaki, 1958–1986. J Clin Epidemiol 44(10):1007–1014
18. Fujiwara S, Kasagi F, Masunari N, Naito K, Suzuki G, Fukunaga M (2003) Fracture prediction from bone mineral density in Japanese men and women. J Bone Miner Res 18(8):1547–1553
19. Kitazawa A, Kushida K, Yamazaki K, Inoue T (2001) Prevalence of vertebral fractures in a population-based sample in Japan. J Bone Miner Metab 19(2):115–118
20. Kasamatsu T, Morioka S, Hashimoto T, Kinoshita H, Yamada H, Tamaki T (1991) Epidemiological study on the bone mineral density of inhabitants in Miyama Village, Wakayama prefecture (Part I). Background of study population and sampling method. J Bone Miner Metab 9(Suppl 1):50–55
21. Kinoshita H, Danjoh S, Yamada H, Tamaki T, Kasamatsu T, Ueda A, Hashimoto T (1991) Epidemiological study on the bone mineral density of inhabitants in Miyama Village, Wakayama prefecture (part II). Bone mineral density of the spine and proximal femur. J Bone Miner Metab 9(Suppl 1):56–60
22. Yoshimura N, Kinoshita H, Danjoh S, Takijiri T, Morioka S, Kasamatsu T, Sakata K, Hashimoto T (2002) Bone loss at the lumbar spine and the proximal femur in a rural Japanese community, 1990–2000: the Miyama study. Osteoporos Int 13 (10):803–808
23. Yoshimura N, Kinoshita H, Danjoh S, Yamada H, Tamaki T, Morioka S, Kasamatsu T, Hashimoto T, Inoue T (1995) Prevalence of vertebral fractures in a rural Japanese population. J Epidemiol 5:171–175
24. Inoue T (1990) Clinical features and findings, osteoporosis (in Japanese). Bone 4:39–47
25. National Osteoporosis Foundation Working Group on Vertebral Fractures (1995) Report assessing vertebral fractures. J Bone Miner Res 10:518–523
26. Genant HK, Wu CY, Van Kujuk C, Nivitt MC (1993) Vertebral fracture assessment using a semiquantative technique. J Bone Miner Res 8:1137–1148
27. Ross PD, Fujiwara S, Huang C, Davis JW, Epstein RS, Wasnich RD, Kodama K, Melton LJ 3rd (1995) Vertebral fracture prevalence in women in Hiroshima compared to Caucasians or Japanese in the US. Int J Epidemiol 24(6):1171–1177

28. Hansen MA, Overgaard, Nielsen VAH, Jensen GF, Gotfredsen A, Christiansen C (1992) No secular increase in the prevalence of vertebral fractures due to postmenopausal osteoporosis. Osteoporos Int 2(5):241–246
29. Jensen GF, Christiansen C, Boesen J, Hegedus V, Transbol I (1982) Epidemiology of postmenopausal spinal and long bone fractures: a unifying approach to postmenopausal osteoporosis. Clin Orthop 166:75–81
30. Harna M, Heliovaara M, Aromaa A, Knekt P (1986) Thoracic spine compression fractures in Finland. Clin Orthop 205:188–194
31. Bengner UU, Johnell O, Redlund-Johnell I (1988) Changes in incidence and prevalence of vertebral fractures during 30 years. Calcif Tissue Int 42(5):293–296
32. Hasserius R, Redlund-Johnell I, Mellstrom D, Johansson C, Nilsson BE, Johnell O (2001) Vertebral deformation in urban Swedish men and women: prevalence based on 797 subjects. Acta Orthop Scand 72(3):273–278
33. Pluijm SMF, Tromp AM, Smit JH, Deeg DJH, Lips P (2000) Consequences of vertebral deformities in older men and women. J Bone Miner Res 15(8):1564–1572
34. Cooper C, Shah S, Hand DJ, Adams J, Compston J, Davie M, Woolf A (1991) Screening for vertebral osteoporosis using individual risk factors. The Multicentre Vertebral Fracture Study Group. Osteoporos Int 2(1):48–53
35. Spector TD, McCloskey EV, Dogle DV, Kanis JA (1993) Prevalence of vertebral fracture in women and the relationship with bone density and symptoms: the Chingford Study. J Bone Miner Res 8(7):817–822
36. Szulc P, Marchand F, Felsenberg D, Delmas PD (1998) Prevalence of vertebral deformities according to the diagnostic method. Rev Rhum Engl Ed 65(4):245–256
37. Grados F, Marcelli C, Dargent-Molina P, Roux C, Vergnol JF, Meunier PJ, Fardellone P (2004) Prevalence of vertebral fractures in French women older than 75 years from the EPIDOS study. Bone 34(2):362–367
38. O'Neill TW, Felsenberg D, Varlow J, Cooper C, Kanis JA, Silman AJ (1996) The prevalence of vertebral deformity in European men and women: the European Vertebral Osteoporosis Study. J Bone Miner Res 11(7):1010–1018
39. Tsai K, Twu S, Chieng P, Yang R, Lee T (1996) Prevalence of vertebral fractures in Chinese men and women in urban Taiwanese communities. Calcif Tissue Int 59(4):249–253
40. Ling X, Cummings SR, Mingwei Q, Xihe Z, Xioashu C, Nevitt M, Stone K (2000) Vertebral fractures in Beijing, China: the Beijing Osteoporosis Project. J Bone Miner Res 15 (10):2019–2025
41. Cummings SR, Melton KJ 3rd (2002) Epidemiology and outcomes of osteoporotic fractures. Lancet 359(9319):1761–1767
42. Office for Lifestyle-Related Diseases Control, Health Services Bureau, Ministry of Health, Labour and Welfare (1998) The trend of dietary circumstances after World War II. Annual report of the national nutrition survey, Japan (in Japanese). Daiichi Shuppan, Tokyo, Japan, pp 145–150
43. Cooper C, Aekinson EJ, O'Fallon WM, Melton LJ 3rd (1992) Incidence of clinically diagnosed vertebral fractures: a population-based study in Rochester, Minnesota, 1985–1989. J Bone Miner Res 7(2):449–456
44. Sanders KM, Pasco JA, Ugoni AM, Nicholson GC, Seeman E, Martin TJ, Skoric B, Panahi S, Kotowicz MA (1998) The exclusion of high trauma fractures may underestimate the prevalence of bone fragility fractures in the community: the Geelong Osteoporosis Study. J Bone Miner Res 13(8):1337–1342
45. The European Prospective Osteoporosis Study Group (2002) Incidence of vertebral fracture in Europe: results from the European Prospective Osteoporosis Study (EPOS). J Bone Miner Res 17(4):716–724
46. Kanis JA, Johnell O, Oden A, De Laet C, De Terlizzi F (2005) Ten-year probabilities of clinical vertebral fractures according to phalangeal quantitative ultrasonography. Osteoporos Int 16 (9):1065–1070

ARTHRITIS & RHEUMATISM
Vol. 54, No. 8, August 2006, pp 2462–2470
DOI 10.1002/art.22041

Contribution of Runt-Related Transcription Factor 2 to the Pathogenesis of Osteoarthritis in Mice After Induction of Knee Joint Instability

Satoru Kamekura,[1] Yosuke Kawasaki,[1] Kazuto Hoshi,[1] Takashi Shimoaka,[1] Hirotaka Chikuda,[1] Zenjiro Maruyama,[1] Toshihisa Komori,[2] Shingo Sato,[3] Shu Takeda,[3] Gerard Karsenty,[4] Kozo Nakamura,[1] Ung-il Chung,[1] and Hiroshi Kawaguchi[1]

Objective. **By producing instability in mouse knee joints, we attempted to determine the involvement of runt-related transcription factor 2 (RUNX-2), which is required for chondrocyte hypertrophy, in the development of osteoarthritis (OA).**

Methods. **An experimental mouse OA model was created by surgical transection of the medial collateral ligament and resection of the medial meniscus of the knee joints of heterozygous RUNX-2–deficient ($Runx2^{+/-}$) mice and wild-type littermates. Cartilage destruction and osteophyte formation in the medial tibial cartilage were compared by histologic and radiographic analyses. Localization of type X collagen and matrix metalloproteinase 13 (MMP-13) was examined by immunohistochemistry. Localization of RUNX-2 was determined by X-Gal staining in heterozygous RUNX-2–deficient mice with the *lacZ* gene insertion at the *Runx2*-deletion site ($Runx2^{+/lacZ}$). Messenger RNA levels of type X collagen, MMP-13, and RUNX-2 were examined by real-time reverse transcriptase–polymerase chain reaction analysis.**

Results. **RUNX-2 was induced in the articular cartilage of wild-type mice at the early stage of OA, almost simultaneously with type X collagen but earlier than MMP-13. $Runx2^{+/-}$ and $Runx2^{+/lacZ}$ mice showed normal skeletal development and articular cartilage; however, after induction of knee joint instability, they exhibited decreased cartilage destruction and osteophyte formation, along with reduced type X collagen and MMP-13 expression, as compared with wild-type mice.**

Conclusion. **RUNX-2 contributes to the pathogenesis of OA through chondrocyte hypertrophy and matrix breakdown after the induction of joint instability.**

Osteoarthritis (OA), a chronic degenerative joint disorder characterized by articular cartilage destruction and osteophyte formation, is a major cause of disability in the elderly. Despite significant demand for more information, risk factors for this disease, as identified by epidemiologic studies, have to date been limited to age, obesity, trauma history, occupation, and sex (1,2). Since these factors are closely related to the accumulation of mechanical loading on joints, mechanical instability of the joints may play some role in OA pathogenesis. In an effort to clarify the mechanisms whereby joint instability leads to the development of OA, experimental animal models of OA induced by producing instability in the joints by surgical intervention have been developed in dogs, rabbits, guinea pigs, and rats (3–9). Due to recent progress in mouse genomics and the availability of transgenic and knockout mice, the mouse is currently the ideal animal for molecular study. Using a microsurgical technique to produce instability in the knee joints of mice, we established models of mechanical instability–induced OA that were reproducible and resembled OA in humans (10).

Supported by a Grant-in-Aid for Scientific Research from the Japanese Ministry of Education, Culture, Sports, Science, and Technology (15209049).

[1]Satoru Kamekura, MD, Yosuke Kawasaki, MD, Kazuto Hoshi, MD, Takashi Shimoaka, MD, Hirotaka Chikuda, MD, Zenjiro Maruyama, MD, Kozo Nakamura, MD, Ung-il Chung, MD, Hiroshi Kawaguchi, MD, PhD: Faculty of Medicine, University of Tokyo, Tokyo, Japan; [2]Toshihisa Komori, MD: Nagasaki University Graduate School of Biomedical Sciences, Nagasaki, Japan; [3]Shingo Sato, MD, Shu Takeda, MD: Tokyo Medical and Dental University, Tokyo, Japan; [4]Gerard Karsenty, MD: Baylor College of Medicine, Houston, Texas.

Address correspondence and reprint requests to Hiroshi Kawaguchi, MD, PhD, Sensory and Motor System Medicine, Faculty of Medicine, University of Tokyo, Hongo 7-3-1, Bunkyo, Tokyo 113-8655, Japan. E-mail: kawaguchi-ort@h.u-tokyo.ac.jp.

Submitted for publication November 24, 2005; accepted in revised form May 16, 2006.

We and other investigators (10–12) have previously reported that the early stage of OA is characterized by hypertrophic differentiation of chondrocytes, as determined by type X collagen expression in the superficial and middle zones of cartilage above the tidemark. Runt-related transcription factor 2 (RUNX-2), which was originally isolated on the basis of its ability to activate transcription of the osteoblast-specific osteocalcin gene (13,14), is known to be the only transcription factor that is required for chondrocyte hypertrophy (15–20). In the present study, therefore, we examined RUNX-2 expression in knee cartilage during OA progression, using our experimental mouse model. In addition, we investigated the functional involvement of RUNX-2 by comparing OA progression in heterozygous RUNX-2–deficient mice with that in wild-type mice.

MATERIALS AND METHODS

Animals. All experiments were performed according to the protocol approved by the Animal Care and Use Committee of the University of Tokyo. For the expression levels of type X collagen, matrix metalloproteinase 13 (MMP-13), type II collagen (CII), and RUNX-2 during OA progression, we used conventional wild-type C57BL/6 mice (8 weeks old) obtained from Charles River Japan (Yokohama, Japan). For the functional analyses of RUNX-2, we used heterozygous RUNX-2–deficient mice ($Runx2^{+/-}$) (129SVJ and C57BL/6 mixed background) that were created as previously reported (21), since homozygous RUNX-2–deficient ($Runx2^{-/-}$) mice died just after birth. $Runx2^{+/-}$ mice and the control wild-type littermates were generated by mating $Runx2^{+/-}$ mice. For the detection of RUNX-2 expression in situ, heterozygous RUNX-2–deficient mice with the *lacZ* gene inserted at the site of the *Runx2* gene deletion in 1 allele ($Runx2^{+/lacZ}$) (CBA and C57BL/6 mixed background) (22) were used (kindly provided by Dr. M. J. Owen, GlaxoSmithKline, London, UK). In total, we used 42 conventional mice, 42 $Runx2^{+/-}$ mice, 42 wild-type mice, and 24 $Runx2^{+/lacZ}$ mice.

OA model. The surgical procedure to create an experimental OA model was performed on 8-week-old mice as previously described (10). Briefly, under general anesthesia using pentobarbiturate (0.5 mg/10 gm body weight, intraperitoneally) (Sigma, St. Louis, MO), the bilateral hind limbs were prepared for aseptic surgery. The knee joint was exposed following a medial capsular incision and gentle lateral displacement of the extensor muscle, without transection of the patellar ligament. Then, the medial collateral ligament was transected, and the medial meniscus was removed using a surgical microscope and microsurgical technique. After replacement of the extensor muscle, the medial capsular incision was sutured, and the skin was closed. During the procedure, close attention was paid not to injure the articular cartilage. A sham operation was performed on the contralateral knee joint using the same approach, with no ligament transection or menisectomy. The animals were then allowed unrestricted activity, food, and water ad libitum.

Histologic analysis. At the indicated time points after surgery, the mice were killed, and the entire knee joints were dissected and fixed for 4 hours at 4°C in 4% paraformaldehyde buffered with phosphate buffered saline (PBS; pH 7.4). The specimens were decalcified for 2 weeks with 10% EDTA (pH 7.4) at 4°C. After the specimens were dehydrated with an increasing concentration of ethanol and embedded in paraffin, 4 μm of the frontal section was cut from the joints. Sections were stained with Safranin O–fast green. Development of OA was quantified by our original histologic grading scale of 0–4 for cartilage destruction (0 = no apparent changes, 1 = loss of superficial zone in articular catilage, 2 = defects limited to above tidemark, 3 = defects extending to calcified cartilage, and 4 = exposure of subchondral bone to cartilage destruction) and 0–3 for osteophyte formation (0 = none, 1 = formation of cartilage-like tissue [cartilaginous outgrowth], 2 = increase in cartilaginous matrix, and 3 = endochondral ossification or osteophyte formation), as previously described (10). The grades were scored as the most severe changes among >20 serial sections. A single observer (KH) who was blinded to the experimental group scored the sections.

Histomorphometric measurements of trabecular bone volume (bone volume/tissue volume) in the subchondral region of medial tibial joints were made according to the guidelines of the American Society of Bone and Mineral Research (23). Measurements of 2 separate sections per knee joint, spaced 50 μm apart, were obtained with an image analyzer (Histometry RT camera; System Supply, Nagano, Japan).

Immunohistochemistry. Immunohistochemical localization of type X collagen, MMP-13, and CII were performed in deparaffinized sections, as previously described (24). The sections were treated with 0.3% H_2O_2 in PBS for 30 minutes and with 2.5% hyaluronidase (Sigma) for 30 minutes. After blocking with 1% bovine serum albumin (Sigma) in PBS for 1 hour at room temperature, sections were incubated with polyclonal rabbit antibodies against rat type X collagen and CII (LSL, Tokyo, Japan), and polyclonal goat antibodies against rabbit MMP-13 (Chemicon, Temecula, CA) at a dilution of 1:100 for 24 hours at 4°C. As negative controls, we used nonimmune rabbit or goat IgG of the same dilution instead of the primary antibodies. The sections were rinsed in PBS and incubated for 20 minutes with Alexa Fluor 488–conjugated goat antibodies against rabbit IgG for type X collagen and with horseradish peroxidase–conjugated goat antibodies against rabbit IgG (ICN Biomedicals, Aurora, OH) for MMP-13 and CII. Visualization of immunoreactivity was performed using Alexa Fluor 488 fluorescence for type X collagen and by diaminobenzidine staining with methyl green counterstaining for MMP-13 and CII.

X-Gal staining. Since neither antibodies nor riboprobes worked appropriately in the localization of RUNX-2 by immunostaining or in situ hybridization of the cartilage tissue of adult mice, respectively, we used X-Gal staining to examine LacZ expression under control of RUNX-2 promoter activation in $Runx2^{+/lacZ}$ mice. Eight-week-old male $Runx2^{+/lacZ}$ mice that underwent the microsurgery described above were killed at 2, 4, and 8 weeks, and the entire knee joint was dissected. The specimens were fixed in 2% paraformaldehyde buffered with PBS (pH 7.4) for 1 hour at 4°C. To detect β-galactosidase activity, the tissues were stained with X-Gal, as previously described (22). The specimens were decalcified for

2 weeks with 10% EDTA (pH 7.4) at 4°C. After dehydration with an increasing concentration of ethanol and embedding in paraffin, 4 μm of the frontal section was cut from the joints.

Real-time reverse transcriptase–polymerase chain reaction (RT-PCR) analysis. To determine the messenger RNA (mRNA) levels of RUNX-2, type X collagen, and MMP-13 in OA cartilage, we collected the medial tibial cartilage from OA and sham-operated knee joints 2, 4, and 8 weeks after surgery, as previously described (25). Total RNA was extracted from the samples using the chaotropic TRIzol method, followed by isogen–chloroform extraction and isopropanol precipitation (Nippon Gene, Tokyo, Japan), according to the manufacturer's instructions. Total mRNA (1 μg) was reverse transcribed using Superscript reverse transcriptase with random hexamer (Takara Shuzo, Shiga, Japan), and 1 μl of each reverse transcriptase reaction was used as a template for the second-step SYBR Green real-time RT-PCR. The full-length or partial-length complementary DNA of target genes, including PCR amplicon sequences, was amplified by PCR, cloned into pCR-TOPO Zero II or pCR-TOPO II vectors (Invitrogen, Carlsbad, CA), and used as standard templates after linearization. QuantiTect SYBR Green PCR Master Mix (Qiagen, Chatsworth, CA) was used for the second-step SYBR Green real-time RT-PCR according to the manufacturer's instructions. SYBR Green PCR amplification and real-time fluorescence detection were performed using an ABI Prism 7700 sequence detection system (Applied Biosystems, Foster City, CA). All reactions were run in quadruplicate. Copy numbers of target gene mRNA in each total RNA were calculated by reference to standard curves and were adjusted to the mouse standard total RNA (ABI) with the mouse actin as an internal control. PCR amplification was performed using the following gene-specific primer pairs: for type X collagen, sense 5′-CATAAAGGGCCCACTTGCTA-3′ and antisense 5′-TGGCTGATATTCCTGGTGGT-3′; for MMP-13, sense 5′-AGGCCTTCAGAAAAGCCTTC-3′ and antisense 5′-TCCTTGGAGTGATCCAGACC-3′; for RUNX-2, sense 5′-CCCAGCCACCTTTACCTACA-3′ and antisense 5′-TATGGAGTGCTGCTGGTCTG-3′; and for actin, sense 5′-AGATGTGGATCAGCAAGCAG-3′ and antisense 5′-GCGCAAGTTAGGTTTTGTCA-3′. Data were normalized by the average mRNA level before the operation (time 0), and expressed as the mean ± SEM in 8–10 mice per group per time point.

Radiographic analysis. Radiographs of the knee joints of wild-type and Runx2$^{+/-}$ mice were obtained 12 weeks after surgery under general anesthesia using a soft x-ray apparatus (CMB-2; Softex, Tokyo, Japan).

Statistical analysis. Group means were compared by analysis of variance, and significance of differences was determined by post hoc testing with Bonferroni adjustment. P values less than 0.05 were considered significant.

RESULTS

Time course of type X collagen, MMP-13, and CII expression in OA cartilage. Among the 4 types of experimental mouse OA models, we used the medial model in this study, with transection of the medial collateral ligament and resection of the medial meniscus of the knee of 8-week-old male mice (10). This model exhibits the disorder in the medial portion, resembling the area most affected by OA in humans, and is suitable for observation of the early stage of OA, since it displays a relatively slow progression of the condition. In fact, Safranin O staining showed matrix degradation at 4 weeks after surgery and cartilage destruction into the middle zone at 8 weeks (Figure 1A).

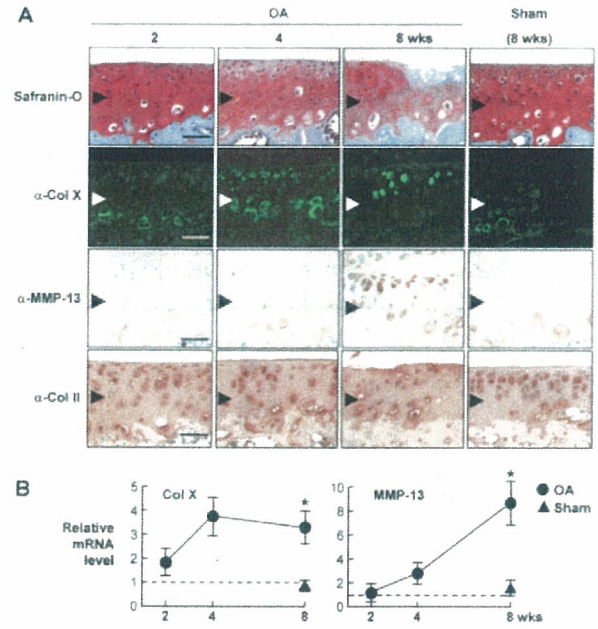

Figure 1. Time course of expression of type X collagen (Col X), matrix metalloproteinase 13 (MMP-13), and type II collagen (CII) in the medial portion of tibial cartilage during the development of osteoarthritis (OA) by induction of joint instability. Eight-week-old male wild-type mice underwent medial collateral ligament transection and medial meniscus resection in the right knee joint, as described in Materials and Methods. A sham operation was performed on the left knee joint, using the same approach. **A,** Representative histologic features of frontal sections of the right knee 2, 4, and 8 weeks after surgery and of the left knee 8 weeks after surgery. Safranin O staining and immunohistochemical staining with type X collagen, MMP-13, and CII antibodies were performed. Immunoreactivity was visualized with Alexa Fluor 488 fluorescence for type X collagen, and with diaminobenzidine staining with methyl green counterstaining for MMP-13 and CII. **Arrowheads** indicate the levels of the tidemark. Bars = 100 μm. **B,** Type X collagen and MMP-13 mRNA levels in medial tibial cartilage extracts from OA and sham-operated knee joints, determined by real-time reverse transcriptase–polymerase chain reaction analysis. Data were normalized to the average mRNA level before the operation (time 0) (set at 1) and are expressed as the mean ± SEM of 8 samples per group per time. * = $P < 0.01$ versus sham-operated knees.

Immunohistochemical analyses were performed

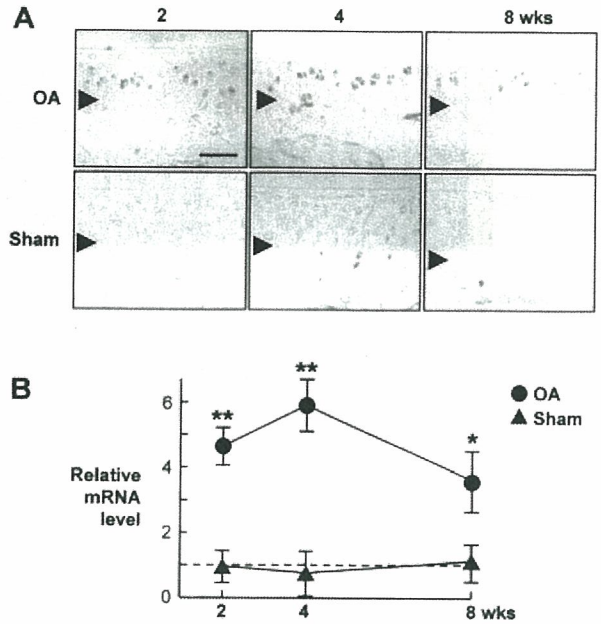

Figure 2. Time course of runt-related transcription factor 2 (RUNX-2) expression in the medial portion of tibial cartilage during development of osteoarthritis (OA) by induction of joint instability. **A,** Representative histologic features of frontal sections 2, 4, and 8 weeks after surgery. For runt-related transcription factor 2 (RUNX-2) expression in situ, 8-week-old male $Runx2^{+/lacZ}$ mice (n = 4 per group per time) underwent microsurgery or sham operation as described in Materials and Methods, and the specimens were stained with X-Gal to detect β-galactosidase activity. **Arrowheads** indicate the level of the tidemark. Bar = 100 μm. **B,** RUNX-2 mRNA level in medial tibial cartilage extracts from OA and sham-operated knee joints of conventional wild-type mice, as determined by real-time reverse transcriptase–polymerase chain reaction analysis. Data were normalized to the average mRNA level before the operation (time 0) (set at 1) and are expressed as the mean ± SEM of 8 samples per group per time. * = $P < 0.05$; ** = $P < 0.01$ versus sham-operated knees.

in this model to assess the time course of type X collagen and MMP-13 expression, which in our previous study (10), were shown to be most strongly induced among collagens and MMPs during OA progression. Although type X collagen expression was limited to the deep calcified zone below the tidemark in the sham-operated knee and at 2 weeks after OA induction, at 4 weeks, it appeared in the superficial and middle zones above the tidemark. MMP-13 expression was not detected above the tidemark at 2 or 4 weeks; however, it was clearly localized in hypertrophic chondrocytes at 8 weeks. The up-regulation of type X collagen and MMP-13 occurred only in the medial portion of the knee joint, where the mechanical instability was loaded, but not in the unaffected lateral portion (data not shown). In contrast, the immunolocalization of CII was unaltered during OA progression, as we previously reported (10). Quantification of mRNA levels in cartilage extracts by real-time RT-PCR analysis confirmed the distinct time course of the expression of type X collagen and MMP-13 (Figure 1B). These findings suggest that articular chondrocytes undergo hypertrophic differentiation in response to joint instability at an early stage, and the hypertrophic chondrocytes express MMP-13, which may degrade the cartilage matrix.

Time course of RUNX-2 expression in OA cartilage. We examined the involvement of RUNX-2, a transcriptional activator that has been known to induce both chondrocyte hypertrophy and MMP-13 expression (15–20,26,27). We initially created the medial OA model in the knee joint of $Runx2^{+/lacZ}$ mice, and examined RUNX-2 expression by X-Gal staining. Time course analysis of the sham-operated cartilage revealed that RUNX-2 expression was positive in some chondrocytes in calcified cartilage below the tidemark, but was not visible in cells above the tidemark (Figure 2A). In contrast, RUNX-2 expression was induced above the tidemark in the OA cartilage as early as 2 weeks, was enhanced at 4 weeks, and decreased thereafter until 8 weeks. This RUNX-2 induction also occurred only in the medial portion of the joint, where the mechanical instability was loaded, but not in the unaffected lateral portion (data not shown). Real-time RT-PCR analysis of cartilage extracts from conventional wild-type mice confirmed the time course of the RUNX-2 mRNA level during OA progression (Figure 2B), suggesting the involvement of RUNX-2 in the early stage of OA.

Effects of RUNX-2 insufficiency on type X collagen and MMP-13 expression in OA cartilage. To determine the involvement of RUNX-2 in the induction of type X collagen and MMP-13 during OA progression, we examined the expression in $Runx2^{+/-}$ mice. The $Runx2^{+/-}$ mice, as well as $Runx2^{+/lacZ}$ mice, showed normal skeletal development and articular cartilage under physiologic conditions (data not shown). We therefore created the medial OA model in 8-week-old mice and compared the expression of type X collagen and MMP-13 in the medial tibial cartilage during OA progression. We first confirmed, by real-time RT-PCR analysis, that RUNX-2 mRNA levels were increased at 4 and 8 weeks after surgery in wild-type mice, while levels at both times were significantly reduced to less than half in $Runx2^{+/-}$ mice (Figure 3B). Immunohistochemical analysis showed that type X collagen expression was visible above the tidemark in the articular cartilage of wild-type mice at 4 and 8 weeks after surgery; however,

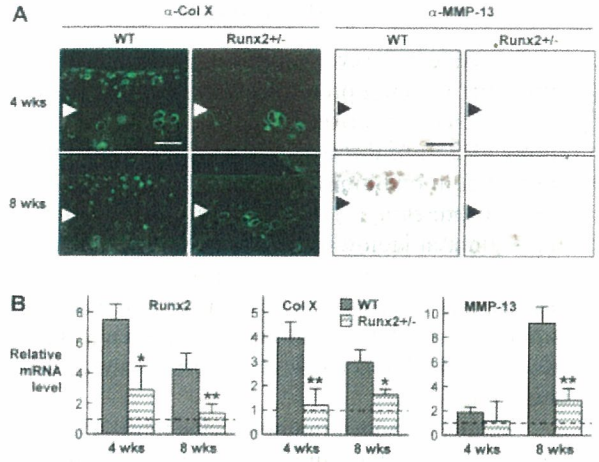

Figure 3. Type X collagen, MMP-13, and RUNX-2 expression in the medial portion of tibial cartilage of wild-type (WT) and $Runx2^{+/-}$ mice during development of OA by induction of joint instability. Eight-week-old male wild-type and $Runx2^{+/-}$ mice underwent microsurgery to induce OA in the knee joints. Samples were prepared and stained as described in Figure 1. **A,** Representative immunohistochemical staining of frontal sections 4 and 8 weeks after surgery. **Arrowheads** indicate the level of the tidemark. Bars = 100 μm. **B,** RUNX-2, type X collagen, and MMP-13 mRNA levels in medial tibial cartilage extracts from wild-type and $Runx2^{+/-}$ mice, determined by real-time reverse transcriptase–polymerase chain reaction analysis. Data were normalized to the average mRNA level before the operation (time 0) (set at 1) and are expressed as the mean and SEM of 8 samples per group per time. * = $P < 0.05$; ** = $P < 0.01$ versus wild-type mice. See Figure 1 for other definitions.

this was rarely seen in the articular cartilage of $Runx2^{+/-}$ mice, except in the calcified cartilage below the tidemark (Figure 3A). MMP-13 expression was also increased above the tidemark in the articular cartilage of wild-type mice at 8 weeks, which was significantly reduced in the cartilage of $Runx2^{+/-}$ mice. Real-time RT-PCR analysis confirmed that both type X collagen and MMP-13 mRNA levels were decreased by RUNX-2 insufficiency (Figure 3B), indicating that chondrocyte hypertrophy and MMP-13 induction during OA progression are at least partly mediated by RUNX-2.

Effect of RUNX-2 insufficiency on OA progression. To further investigate the contribution of RUNX-2 to the development of OA, we next compared the susceptibility of cartilage destruction and osteophyte formation between joints from wild-type and $Runx2^{+/-}$ mice, using joint instability in the medial model. Safranin O staining of cartilage in wild-type mice showed that cartilage destruction progressed into the middle zone by 8 weeks after surgery and reached the calcified cartilage layer across the tidemark by 12 weeks (Figure 4A). The cartilage destruction in $Runx2^{+/-}$ mice was much milder, however, and it was confined within the middle zone throughout the observation period. The $Runx2^{+/lacZ}$ joint was confirmed to exhibit cartilage destruction similar to that of $Runx2^{+/-}$ mice and milder than wild-type mice. Quantification by our original grading system (10) revealed significant reduction of cartilage destruction by the RUNX-2 insufficiency at 8 weeks and thereafter (Figure 4B).

Osteophyte formation, the other characteristic feature of OA, was detected at the medial edge of the joints of wild-type mice 12 weeks after surgery in both radiographic (Figure 5A) and histologic (Figure 5B) analyses. Joints in the $Runx2^{+/-}$ and $Runx2^{+/lacZ}$ mice showed decreased cartilaginous outgrowth and osteo-

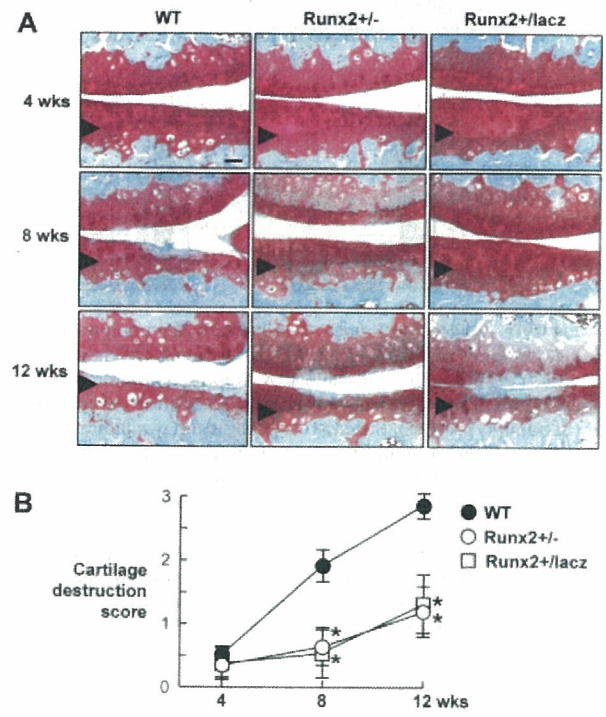

Figure 4. Time course of cartilage destruction in the medial portion of tibial cartilage of wild-type (WT), $Runx2^{+/-}$, and $Runx2^{+/lacZ}$ mice after induction of joint instability. Eight-week-old male mice underwent microsurgery to induce osteoarthritis in the knee joints, and the samples were prepared and stained. **A,** Representative histologic features (Safranin O staining) of frontal sections 4, 8, and 12 weeks after surgery. **Arrowheads** indicate the level of the tidemark. Bar = 100 μm. **B,** Histologic scoring of cartilage destruction according to the grading system described in Materials and Methods. Data are expressed as the mean ± SEM of 10 samples per genotype per time for wild-type and $Runx2^{+/-}$ mice, and of 4 samples per time for $Runx2^{+/LacZ}$ mice. * = $P < 0.01$ versus wild-type mice.